CORTEX
Manuscript Draft

Manuscript Number: CORTEX-D-17-00148

Title: Strategic adaptation to non-reward prediction error qualities and contextual volatility in fMRI

Article Type: Research Report

Keywords: fMRI; expectation; prediction error; sequence learning; top-down control

Abstract: Prediction errors are deemed necessary for the updating of internal models of the environment, prompting us to stop or assert current action plans and helping us to adapt to environmental features. The aim of the present study was twofold: First, we sought to determine the neural underpinnings of qualitatively different abstract prediction errors in a serial pattern detection task. Distinct frontoparietal circuits were found for sequential terminations (inferior frontal gyrus and intraparietal sulcus) and extensions (superior frontal sulcus, posterior cingulate cortex, and angular gyrus), respectively. These findings provide a novel approach of distinguishing non-reward prediction error signals with regard to behavioural consequences they entail.

Second, we investigated predictive processing as a function of statistical context (volatility). We hypothesised that the prospective range of model-based expectancies is adapted to the stability of respective contexts in such a way that unstable environments call for more frequent comparisons of expectancies with sensory input, resulting in stepwise predictions. Changes in environmental stability resulted in activation of the temporoparietal junction and inferior frontal gyrus for the highly volatile context at potential points of prediction violation (checkpoints). Notably, this effect was not due to local fluctuations in stimulus improbability (surprise). Data point towards a context-dependent adaptation of predictive strategies. Conceivably, enhanced BOLD responses at sequential checkpoints reflect stepwise rather than a full-length prediction. This strategic adjustment presumably relies on the iterant evaluation of model information retrieved from working memory, as suggested by strengthened functional connectivity of the parahippocampal area during epochs of high volatility.

Corresponding author: Daniel S. Kluger

Title page

Full manuscript title

Strategic adaptation to non-reward prediction error qualities and contextual volatility in fMRI

Short manuscript title

Abstract PE qualities and adaptive prediction

Key words

fMRI, expectation, prediction error, sequence learning, top-down control

Full names and affiliations

Daniel S. Kluger[a,b] and Ricarda I. Schubotz[a,b,c]

[a] Department of Psychology, University of Muenster, Muenster, Germany

[b] Otto-Creutzfeldt-Center for Cognitive and Behavioral Neuroscience, University of Muenster, Muenster, Germany

[c] Department of Neurology, University Hospital Cologne, Cologne, Germany

The reported work was performed at

Department of Psychology
University of Muenster
Fliednerstr. 21
D-48149 Muenster
Germany

Correspondence should be addressed to

Daniel S. Kluger
Department of Psychology
University of Muenster
Fliednerstr. 21
D-48149 Muenster
Germany
Telephone: 0049-251-8334101
E-mail: daniel.kluger@uni-muenster.de

Abstract

Prediction errors are deemed necessary for the updating of internal models of the environment, prompting us to stop or assert current action plans and helping us to adapt to environmental features. The aim of the present study was twofold: First, we sought to determine the neural underpinnings of qualitatively different abstract prediction errors in a serial pattern detection task. Distinct frontoparietal circuits were found for sequential terminations (inferior frontal gyrus and intraparietal sulcus) and extensions (superior frontal sulcus, posterior cingulate cortex, and angular gyrus), respectively. These findings provide a novel approach of distinguishing non-reward prediction error signals with regard to behavioural consequences they entail.

Second, we investigated predictive processing as a function of statistical context (volatility). We hypothesised that the prospective range of model-based expectancies is adapted to the stability of respective contexts in such a way that unstable environments call for more frequent comparisons of expectancies with sensory input, resulting in stepwise predictions. Changes in environmental stability resulted in activation of the temporoparietal junction and inferior frontal gyrus for the highly volatile context at potential points of prediction violation (*checkpoints*). Notably, this effect was not due to local fluctuations in stimulus improbability (*surprise*). Data point towards a context-dependent adaptation of predictive strategies. Conceivably, enhanced BOLD responses at sequential checkpoints reflect stepwise rather than a full-length prediction. This strategic adjustment presumably relies on the iterant evaluation of model information retrieved from working memory, as suggested by strengthened functional connectivity of the parahippocampal area during epochs of high volatility.

Introduction

In attempting to make sense of incoming sensory event information in everyday life, we are constantly faced with discrepancies between our internal model of the world and the information we actually obtain (Rao & Ballard, 1999). In predicting future events, the brain efficiently processes predictable portions in perceptual information: only if incoming sensory signals differ from higher-level predictions is the corresponding error signal propagated "upward" to the next highest stage of the processing hierarchy (Mumford, 1992; Friston, 2005). Such prediction errors inarguably differ with regard to their quality and the behavioural consequences they entail: when walking down a familiar flight of stairs, one might occasionally over- or underestimate the remaining number of stairs on the bottom landing, evoking qualitatively different moments of surprise. Furthermore, context will likely influence the way in which we make assumptions about upcoming events: we will compare our expectations with reality more frequently in noisy or unfamiliar contexts, for instance when carrying a fridge through the same staircase in dim lighting.

Research on definitive features of these prediction errors has predominantly been directed towards quantitative rather than qualitative differences between neural error signals. For instance, the concept of *surprise* (Jones, 1979), cast to reflect the improbability of a particular event, has been demonstrated to modulate prediction errors in that more surprising expectancy violations elicit stronger error signals (Strange, 2005; Egner et al., 2010). However, aside from a few studies in the cognitive domain (e.g. den Ouden et al., 2010; Schiffer et al., 2012), imaging efforts to classify *qualitatively* different types of such prediction errors have so far been restricted to contexts involving a reward component. Here, findings from animal studies (Bayer & Glimcher, 2005) and gambling tasks in humans (Delgado et al., 2003) have demonstrated a functional distinction of *positive* and *negative* reward prediction errors based on whether an obtained reward value was higher or lower than expected, respectively (Schultz et al., 1998).

In contrast, such distinctive characteristics of prediction errors are considerably less well understood in absence of external reward. In light of the immediate importance of error signals for internal model updating (e.g. Bastos et al., 2012) and adequate action selection, however, the need to understand the qualities of more abstract prediction errors becomes evident: as prediction errors are thought to be the foundation of learning mechanisms (den Ouden, 2009), different types of expectancy violations might result in qualitatively distinguishable prediction error signals and - consequently - in distinct modifications of upcoming expectancies and behaviour. Recall that short term predictions are used to facilitate perception when we observe structured regularities such as sequential events. When these regularities end earlier than expected, the appropriate adaptation would be to reject the now invalid predictive model in favour of a more *externally* driven mode of tracking incoming information. In contrast, any regularity we perceive may as well persist longer than expecte. Accordingly, such an unexpected extension would then call for a resumption of the *internally* driven mode of model-based prediction.

As much as this reactive, local adaptation of stimulus processing and behaviour should reflect different types of prediction errors, it should likewise depend on global, higher order characteristics of the environment. Exploring the nature of error signals and their effects on model adaptation therefore raises the question of whether predictive strategies remain constant across contexts. The measure of v*olatility* refers to the variability of informational value over time and therefore reflects higher-order statistical features of the environment. Within the scope of reward-related paradigms, volatility has been shown to induce uncertainty in current reward expectancy (Rushworth & Behrens, 2008). While overall processing of context volatility has been linked to activity in the anterior cingulate cortex (ACC) as a function of reward prediction error computation (Behrens et al., 2007; Silvetti et al., 2013), implications of context (in)stability on abstract prediction still remain unclear. Conceivably, memory-driven internal models of future sensory information might be adapted to the volatility of respective contexts. In stable contexts of low volatility, prediction errors can be conceived of as more meaningful in that they are highly informative with regard to potential benefits

of model adaptation (i.e. learning). In contrast, prediction errors in statistically unstable (i.e. highly volatile) contexts carry less information contributing to learning-related gains. Predicting upcoming events can be considered an investment in the sense that false predictions inevitably lead to costly adjustments of forward models (Clark, 2013). Therefore, depending on how reliably forward models can be used to predict future events (as conveyed through statistical learning of environment regularities), it may be more efficient to employ a strategy of partial or stepwise short-term predictions rather than predicting consecutive events at full length. For example, as opposed to preparing a complete model of an expected sequence of events, a stepwise prediction might imply an iterative monitoring of sequence continuation at particular sequential positions. Most likely to serve as such *checkpoints* would be those points in time where breaches of expectancy had previously been observed. This way, statistical learning might be employed to adapt predictive strategies to particular informational structures in the environment. Support for this hypothesis comes from studies linking the working memory network (most prominently hippocampus and adjacent areas) to both the predictive processing of sequential patterns (Lisman, 2009; Fortin et al., 2002; Rolls, 2013) as well as the decoding of contextual information (Allen et al., 2014; Davachi & DuBrow, 2015).

We conducted the present fMRI study to assess qualitative differences between prediction error signals and the influence of volatility on predictive strategies using an implicit cueing paradigm. Participants were asked to detect short or long ordered digit sequences (5 and 7 items, respectively) within an otherwise pseudorandom stream of single digits. They indicated the onset of a detected sequence by an immediate button press and the sequence ending by button release. The expected sequence length, as implicitly cued by digit colour (see Material and Methods), was occasionally violated by terminations and extensions. Thus, whereas the task was overtly concerned with sequence detection, our analysis was focussed on specific events during or at the end of sequences.

As to our first hypothesis, we expected distinguishable neural correlates to reflect the respective reorientation towards external stimuli (sequential terminations) or towards the internal model derived from working memory (sequential extensions). Particularly, the unexpected need to stay with the internal model as induced by sequential extensions was expected to elicit higher activation within posterior cingulate cortex (PCC), a region previously hypothesised to reflect memory-driven cognition (Raichle et al., 2001, Leech et al., 2012). Conversely, the unexpected need to disregard the currently employed internal model as induced by sequential terminations was hypothesised to engage the inferior frontal gyrus (IFG), an area that has been reported for violations of ordered pattern expectancy across domains (Fiebach & Schubotz, 2006).

Second, we assessed the effects of context volatility on predictive strategies by manipulating the proportion of violated sequences over time. Neural activity at checkpoint positions was expected to be elevated in highly volatile contexts, thus indicating a stepwise prediction mode. Due to its established role in reward-related volatility monitoring (Behrens et al., 2007), we assumed ACC to represent higher-level context information necessary to initiate stepwise predictions in highly volatile environments. Crucially, these global fMRI effects were controlled for potential confounds by varying levels of stimulus-bound surprise (i.e. the extent to which individual stimuli were locally unexpected). To this end, we employed a parametric regressor of nuisance reflecting a stimulus' respective surprise value, thus allowing us to disentangle higher level context effects from mere differences in improbability.

Material and Methods

Participants

A total of 22 neurologically healthy, right-handed volunteers (13 female, mean age: 24.3 (20 – 30) years) participated in the study. Participants were recruited from the university's volunteer database and had normal or corrected-to-normal vision. Colour blindness was ruled out using Ishihara colour test plates (Ishihara, 1917). Written informed consent was obtained from each participant prior to the start of experimental procedures. Experimental standards complied with the local Ethics Committee of the University of Münster. Participants selectively received payment or course credit as compensation for their participation in the study. Two participants were excluded from further data analysis due to poor behavioural performance and self-reported tiredness during the experiment (see below). Therefore, all reported analyses of functional data are based on a population of 20 participants (12 female, mean age 24.8 (21 - 30) years).

Stimulus material

The stimuli consisted of pseudorandomly coloured single digits (0 – 9, size 1.5° of visual angle) presented individually for 500 ms in the centre of a light grey computer screen (see Fig. 1A). Digits were presented in blocks with a length of approximately 6 min (range of trial numbers: 736 – 738, see "Experimental procedures" for details). Numbers of presentations for all colours and digits were equally distributed both within and across blocks. Each block contained *sequential trials* (i.e. digits with a recognisable relation to the preceding one) as well as *random trials* (i.e. digits that were not discernibly related to either the preceding or the following digit). Sequential trials in turn belonged to one of two types of sequences: *ordered sequences* constantly increased the preceding figure by one (e.g. 5 – 6 – 7 – 8 – 9; Fig. 1A, left). In order to allow for ordered sequences to start on any figure, the ascending regularity necessarily included the 0 character and was thus continued in a circular fashion

after the figure 9 (e.g. 8 – 9 – 0 – 1 – 2). *Colour sequences* were defined as consecutive trials all presented in the same colour (dark red). Importantly, the numerical values during colour sequences were pseudorandom (Fig. 1A, right). Therefore, at no point was there a succession of continuously ascending figures presented in the same colour, but only one sequential condition at a time (i.e. ordered or colour). Colour sequences were employed to ensure a high level of attentiveness and were not a pivotal subject to our analyses. Random trials included neither self-repetitions nor immediately adjacent figures and therefore could not be mistaken for ordered sequences.

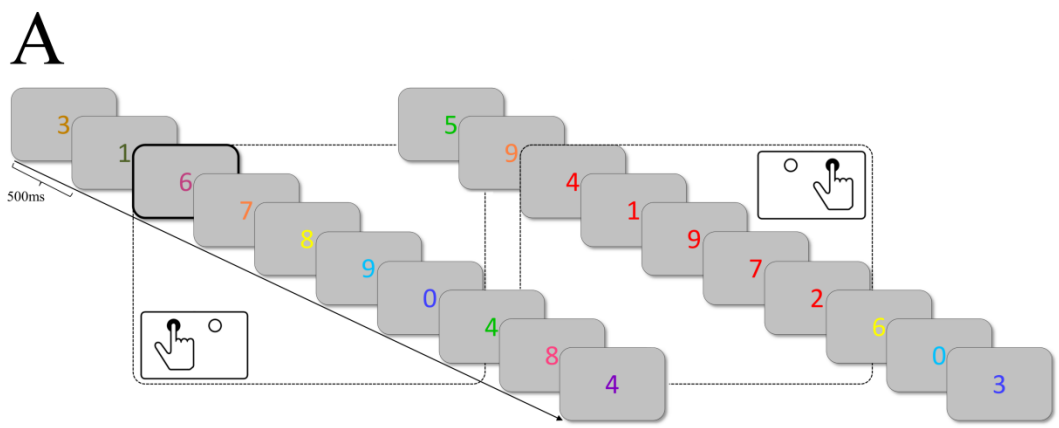

Figure 1. (A) Exemplary trial successions and time windows of respective corresponding responses for ordered (left) and colour sequences (right). Cue trial for the ordered sequence has been highlighted (bold black frame) for illustrative purposes. (B) Cue-based expected sequence length and resulting prediction errors for terminated, regular, and extended short ordered sequences (*expectation compliance*). Based on the cue (in this case, a magenta figure), five regularly ascending figures are expected. Cue trial has been highlighted for illustrative purposes. Top: terminated sequences are shortened by two trials and therefore induce a prediction error (predicted sequence > presented sequence). Middle: regular sequences match the cue-based expected sequence length (predicted sequence = presented sequence), hence no prediction error arises. Bottom: extended sequences are prolonged by two trials and therefore induce a prediction error (predicted sequence < presented sequence).

Undisclosed to the participants, two colours were used as cues to indicate the onset of ordered sequences: one colour marked the first digit of a *short* ordered sequence (regular length of five digits), a second colour marked the first digit of a *long* ordered sequence (regular length of seven digits). Each participant was assigned two individual cue colours which did not belong to the same hue. Cue validity was fixed at p = .80 throughout the experiment with invalid cues being followed by a random figure instead of the next higher one (as would have been suggested by the cue). Neither one of the cue colours nor the red hue used for the colour sequences appeared during random trials. Importantly, the colour cues were employed to trigger predictions with regard to the length of the to-be-observed sequence and were not analysed as events of interest themselves.

In order to induce prediction errors based on the implicit information conveyed by the colour cues, ordered sequences were manipulated in terms of their *expectation compliance.* This factor was introduced to distinguish between *regular*, *terminated*, and *extended* ordered sequences. Given the regular length of five and seven figures, respectively, terminated sequences were shortened by two items (e.g. three instead of five figures for short ordered sequences) while extended sequences were equally prolonged by two items (e.g. seven instead of five figures for short ordered sequences). A graphic display of expected sequence length and expectation compliance is shown in Figure 1B.

Finally, the composition of regular, terminated, and extended sequences within a particular block was varied across blocks. This way, the *volatility* of the blocks (i.e. the frequency of change with regard to cue-based expectations) was set to be either *high* or *low*. Blocks of low volatility featured local probabilities of p_{reg} = .70 for the regular configuration and $p_{term/ext}$ = .15 for both terminated and

extended sequences. These blocks could therefore be seen as statistically stable regarding cue-based expectations. Local probabilities for terminated and extended sequences were always identical for both sequence lengths. Highly volatile blocks, in contrast, corresponded to a more unstable statistical structure regarding the expectation based on the cue. Local probabilities after the cue during highly volatile blocks were p_{reg} = .40 and $p_{term/ext}$ = .30. It is important to note that at any point during the experiment the regular configuration was the statistically most likely continuation of the sequence. An overview of the statistical structure following the volatility factor is provided in Figure 2, please see the Supplementary Material (Fig. S1) for details on the composition of experimental blocks.

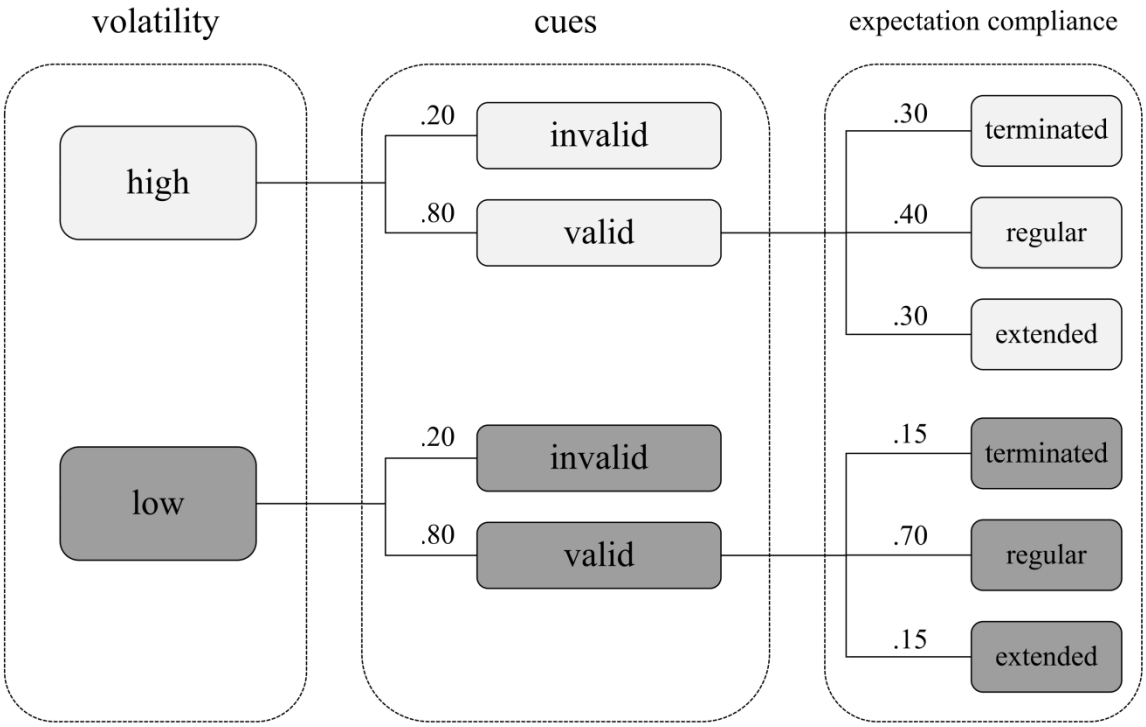

Figure 2. Local transition probabilities for terminated, regular, and extended sequences depending on the respective block volatility. Note that only the composition of expectation compliance levels varied with volatility while cue validity itself remained fixed across blocks.

Starting points of all sequences were balanced across digits. Successions of random trials were equally distributed within a range of 5 – 9 digits (*M* = 7.19 digits) both within and across blocks. To ensure an even distribution of colour presentations, a total of 29 different colours were used. The

colours employed in the present study had been validated in a behavioural pilot study (n = 18) to ensure equal visibility of all colours.

Tasks

Participants were asked to indicate detection of ordered sequences as well as colour sequences by corresponding button presses. Therefore, they were instructed to press the left button with their right index finger as soon as they noticed an ordered sequence and to hold the button for the duration of the sequence. Accordingly, release of the left mouse button was to indicate the end of the ordered sequence (i.e. the onset of subsequent random trials). Equivalently, participants were instructed to press and hold the right mouse button with their right middle finger to indicate detection of a colour sequence. Once again, release of the right mouse button marked the end of a colour sequence. A mouse was used in the behavioural sections (i.e. introductory trials, training, and post-measurement) to closely match responses with the two-button response box used during the fMRI session (see below).

Experimental procedures

The study was conducted on two consecutive days. The first day appointment was laid out as a training session in order to allow participants to familiarise themselves with the task and to provide them with implicit knowledge concerning the cues and the underlying statistical structure of the experiment. Importantly, at no point during the training or the fMRI session was it revealed that there was informational content in some of the colours (i.e. the cues) or that the blocks varied in their respective statistical structure (i.e. their volatility). The second day included the fMRI session as well as a subsequent post-measurement. The experiment was programmed and run using the Presentation 14.9 software (Neurobehavioral Systems, San Francisco, CA, USA).

Day 1 (training session)

After having been informed about the very general scope of the study ("digit processing", supposedly), participants completed a first introduction to the task. Participants were presented with a stimulus stream of 130 digits (overall duration 65 s) including exactly one presentation of each ordered sequence configuration (i.e. terminated, regular, and extended sequences of both lengths), one invalid cue of each sequence length as well as one motor control sequence. Length range and proportion of random trials were matched with the behavioural and the fMRI experiment. Responses were not recorded during the introductory trials and participants were allowed to repeat the introduction until they felt comfortable with the task.

The training consisted of two blocks (one block of high and low volatility, respectively) with a total of 1463 digits (duration approx. 12 min – for precise trial formation, see section "Stimulus material"). Block order was balanced across participants. Length range and proportion of random trials were matched with the fMRI experiment. After the completion of a block, participants were encouraged to take some time and grant themselves a short break before continuing with the next block.

Day 2 (fMRI session and post-measurement)

Participants once again completed the introductory phase from the previous day in a quiet working environment immediately before entering the scanner. The following fMRI session consisted of four blocks (two blocks of both high and low volatility, respectively) with a total of 2949 digits (duration approx. 24 min). Contrary to the training, participants were presented with a screen notifying them of a short break for ten seconds after completion of a block. Experimental procedure and task during the fMRI session were otherwise identical to the training session.

Following the functional scanning, participants completed a behavioural post-measurement in order to assess their implicit knowledge of the cue information. To this end, they were presented with one block of 620 digits (duration approx. 5 min) shown on a computer. Length range and proportion of random trials were matched with the training session and the fMRI experiment. Participants were

asked to perform the identical task as before (i.e. to indicate sequence detection by button press). Crucially, only half of the ordered sequences were cued by the same colours as during the training and the fMRI session. The other half began with fixed, but different colours that had indeed been presented during training and fMRI, but not as cues for the respective participant. Therefore, they contained no implicitly learned information concerning upcoming trials. As with the established cue colours, two previously non-informative colours were assigned to mark the beginning of short and long ordered sequences, respectively.

Finally, participants were interviewed verbally to assess whether they were aware of the presence of the colour cueing. They were asked whether they had noticed any regularity at all with regard to the digits' colours. All participants denied having noticed any colour-related regularity.

Behavioural data analysis

Statistical analyses of behavioural responses were performed using R statistical software (R Foundation for Statistical Computing, Vienna, Austria). If not stated otherwise, an α-level of .05 was defined as a statistical threshold.

First, correct and incorrect responses were aggregated separately for training, fMRI session, and post-measurement for each participant. Incorrect responses were further divided into misses and false alarms. Participants' overall performances were assessed via the discrimination index PR (Snodgrass & Corwin, 1988), defined as the difference between hit rate and false alarm rate: correctly reported sequences (i.e. ordered or colour sequences) relative to all sequences was defined as the hit rate. The false alarm rate was defined as falsely reported sequences (again, ordered or colour sequences) relative to all sequences. No specific timeout criterion was defined for the onset of button presses, i.e. responses were registered throughout the whole length of the respective sequence.

Reaction times for button presses (onset latency) and releases (offset latency) were assessed for fMRI session and post-measurement. Latencies were aggregated separately for the levels of *expectation compliance* (terminated, regular, extended) and *volatility* (high, low) as well as for established vs new cue colours, respectively. Aggregation was executed for each participant individually. Onset latency was calculated as reaction time relative to the onset of the second trial of any particular ordered sequence: the second trial of the sequence was the earliest possible point to detect a sequential pattern, since the current trial always had to be compared to the preceding one (i.e., to check whether the figure had risen by 1). Offset latency was calculated as reaction time relative to the onset of the first random trial after any particular sequence. Repeated-measures analyses of variance (ANOVA) and paired *t*-tests were used to assess possible differences in offset (depending on expectation compliance and volatility) and onset latency (learned vs new cue colours during post-measurement), respectively. Results of the paired *t*-tests were corrected for multiple comparisons at $p = .05$ using the false discovery rate (fdr) correction by Benjamini & Hochberg (1995).

Functional data analysis

fMRI data acquisition and data preprocessing

Functional and structural imaging data were collected using a 3T Siemens Magnetom Prisma MRI scanner (Siemens, Erlangen, Germany) equipped with a 20-channel head coil. Participants lay supine with their right hand placed on a two-button response box. Index and middle finger were placed on the two response buttons, matching the response contingencies from the training session. Participants' arms were stabilised on form-fitting cushions and foam padding around the head was applied to prevent motion artefacts. Earplugs and noise-cancelling headphones were provided to reduce scanner noise.

During functional imaging, 30 x 4 mm axial slices (1 mm spacing, 64 x 64 voxel matrix, 192 x 192 mm field of view, resulting voxel size 3 x 3 x 5 mm) were acquired parallel to the bi-commissural line (AC-PC) using a single-shot gradient echo-planar imaging (EPI) sequence sensitive to BOLD contrast (TR = 2000 ms, TE = 30 ms, 90° flip angle, ascending recording, 800 repetitions). Prior to the functional session, a high-resolution structural scan was recorded for each participant using a standard Siemens 3D T1-weighted whole brain MPRAGE imaging sequence (1 x 1 x 1 mm voxel size, TR = 2130 ms, TE = 2.28 ms, 256 x 256 mm field of view, 192 sagittal slices).

Data processing was done with the Lipsia software package (Lohmann et al., 2001). Functional data were spike-corrected (using interpolation with adjacent time points) to reduce artefacts within time series. Correction for slice acquisition time (using cubic spline interpolation) and head motion (3 translation, 3 rotational parameters) was applied and functional data were co-registered with the structural scan (using rigid transformation). Individual structural scans were normalised to the MNI template via general affine transformation and resulting parameters were applied to the functional scans. The resulting normalised functional images were resampled to 3 mm isotropic voxels, high-pass filtered with a 100 s period cutoff and spatially smoothed with an 8 mm full-width half-maximum (FWHM) Gaussian kernel.

fMRI analysis

Event-related BOLD responses were estimated in a general linear model (GLM) approach. The GLM was constructed to test for distinct neural correlates of the different error types as well as for effects of statistical block structure on neural processing at different time points during ordered sequences. Additionally, the parametric effect of surprise was modelled to control for trial-by-trial variation in stimulus improbability. Therefore, the model comprised a total of seven regressors of interest reflecting the 3 x 2 combination of the factors *expectation compliance* (terminated, regular, extended) and *volatility* (low, high) plus the surprise parameter. For terminations, the event onset was time-locked to the first unexpected *random* digit (i.e. the fourth [short sequences] or sixth [long

sequences] sequential position, respectively; see Fig. 1B). Equivalently, extensions were modelled with the onset time-locked to the first unexpected *sequential* digit (i.e. the sixth [short] or eighth [long] sequential position, respectively). Regular events (termed *checkpoints*) were defined as points in time at which we hypothesised the incoming stimulus to be checked for either a termination (i.e. a check occurring during the ongoing sequence) or an extension (i.e. a check at the regular end) of the ordered sequence. Importantly, checkpoints were only classified as such when the ordered sequence was in fact continued as indicated by the cue, that is, in the regular configuration (see Fig. 3 for an example and Supplementary Fig. 1 for details on event specification). In case the current stimulus did not match the prediction, the event was classified as a prediction error instead of a checkpoint.

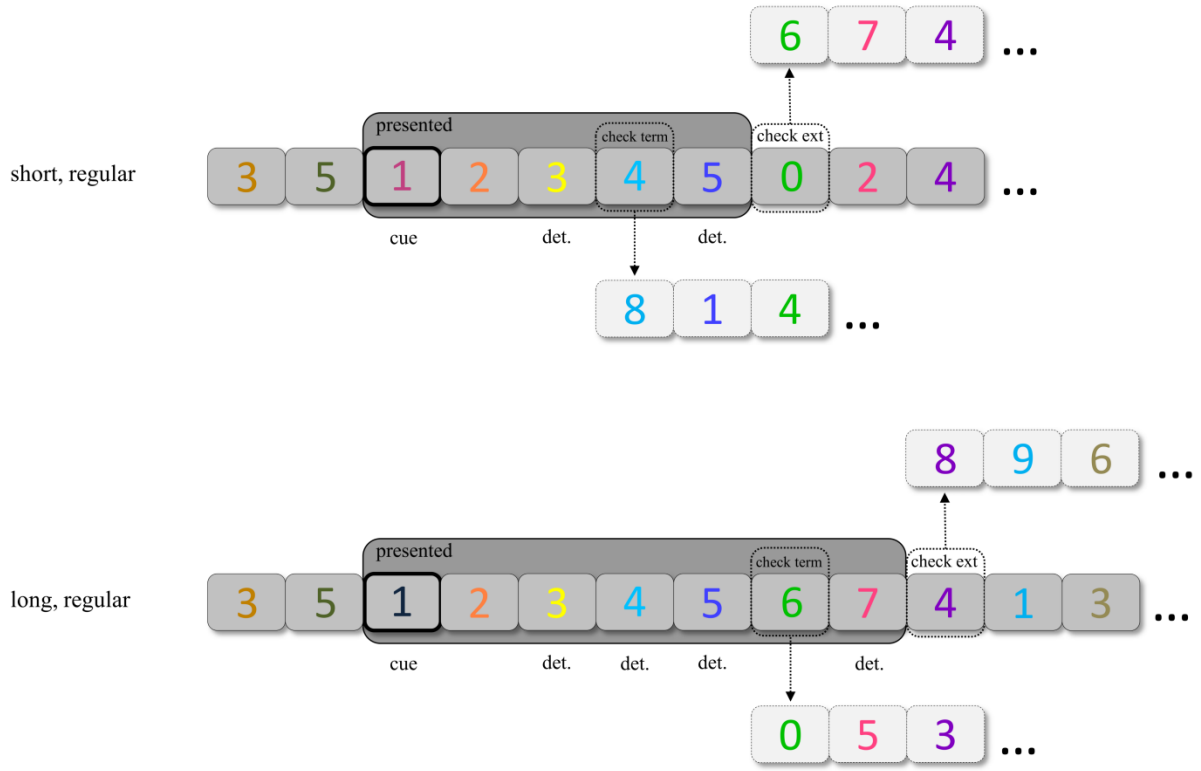

Figure 3. Illustration of checkpoints during a regular short and long ordered sequence, respectively. As indicated by the cue (highlighted for the purpose of this graphic), five or seven consecutive digits following the +1 rule are presented. Two checkpoints are hypothesised over the course of each sequence: For instance, during short ordered sequences (top), the fourth item can be used to check whether the sequence is terminated (check term) or not. A hypothetical course of a terminated sequence is outlined (lower trial succession, dashed framing). The sixth item (i.e. the first random figure after the regular short ordered sequence) can be used to check for an extension of the sequence (check ext). A hypothetical course of an extended sequence is outlined (upper trial succession, dashed framing). Within a particular ordered sequence, checkpoints are always preceded by deterministic items (det.).

With respect to difference characteristics, one could justifiably argue that the difference between checkpoints and prediction errors may not at all be qualitative, but rather a quantitative excess of prediction errors with regard to their respective improbabilities. From this point of view, checkpoints could be construed as muted prediction error signals with a lesser degree of surprise. While surprise inarguably modulated cognitive processing in the present task, our key point of suggesting a functional role for checkpoints was to gain insight into qualitatively different processing of regular events depending on the particular context. By including a parametric surprise regressor, we attempted to discriminate between these qualitative effects and quantitative distinctions that can be ascribed to mere differences in improbability.

The parametric effect of surprise was estimated following the notion of an ideal Bayesian observer (see Harrison et al., 2006). Event-specific surprise $I(x_i)$ was defined as the improbability of event x_i, i.e.

$$I(x_i) = -\ln p(x_i)$$

with

$$p(x_i) = \frac{n_j^i + 1}{\sum_k n_k^i + 1}$$

where n_j^i denotes the total number of occurrences of outcome *j* (*terminated, regular, extended*) up to the current observation *i* relative to the sum of all past observations (with *k* for all possible outcomes). Colour sequences and breaks during the experiment were modelled as regressors of nuisance in order to account for variance unrelated to the events of interest. All correlations between non-parametric regressors of the design matrix were lower than r = .20; therefore, we did not perform regressor orthogonalisation.

Contrast specification

The main effect of *expectation compliance* was assessed by the second-level contrast of terminated and extended sequences (TERM > EXT). Common activations of both error types were assessed by the conjunction of the two single contrasts vs checkpoints, respectively (i.e. TERM > CHECK ∩ EXT > CHECK). Note that due to the probabilistic structure of the task, there were considerably more checkpoints than prediction errors contributing to the respective regressors (ratio ~ 2:1). Therefore, for the conjunction of TERM > CHECK and EXT > CHECK, we constructed a parallel GLM identical to the one described above, with the one exception that only half of the checkpoint events were included in the respective regressors of the second model. While this approach resulted in reduced power of the respective contrasts and their conjunction, its merit lies in a markedly well-balanced, less biased contrast of conditions.

The effects of *volatility* on checkpoint and prediction error processing were assessed by the contrasts of high vs low volatility checkpoints (CHECK_HIGH > CHECK_LOW) and prediction errors (PE_HIGH > PE_LOW, data not shown), respectively.

For group level analyses, one sample t-tests were calculated using first-level contrast images of all subjects. Resulting t-values were converted to z-scores and thresholded at voxel-wise $p < .001$. In a second step, this initial thresholding was combined with a cluster-extent based threshold derived from Monte Carlo Simulation (see Forman et al., 1995). We ran 5000 iterations using the fMRIMonteCluster tool (available at github.com/mbrown/ fmrimontecluster), yielding a cluster-extent based threshold of $k > 783$ mm^3 (29 contingent voxels, cluster-level $p < .05$).

Exploratory functional connectivity analysis

When investigating the interplay of brain regions in forming coactivation networks, functional connectivity measures have become increasingly popular to complement BOLD amplitude effects of participating brain regions. Eigenvector centrality mapping (ECM) has been proposed by Lohmann

and colleagues (2010) as a graph-based means to determine the centrality of neural structures within their respective networks. Particularly, eigenvector centrality (Bonacich, 2007) refers to how strongly a certain structure (a *node,* in terms of graph theory) is functionally connected to other highly interconnected nodes. Therefore, both number and quality of connections are factored into the centrality value assigned to a particular voxel. Since the interesting aspect here was precisely to evaluate the influence of volatility on the neural processing within task-related networks (whose components are themselves highly interconnected), ECM was explicitly well suited for the functional connectivity analysis at hand. Importantly, ECM does not depend on a priori assumptions and, due to computational efficiency, allows for functional connectivity analyses of the entire brain. Finally, ECM does not require parameter adjustments other than the definition of the voxel space and the time period of interest.

In order to assess potential effects of volatility on functional connectivity, eigenvector centrality was analysed post-hoc within a whole-brain mask (≈ 60 000 voxels). To avoid connectivity changes caused by the mere duration of scanner time (see Lohmann et al., 2010), ECM analysis was restricted to the first half of the experiment (i.e. one block of each volatility level in counterbalanced order) for each participant. Pairwise similarity matrices for time series of any two voxels were computed and subsequently analysed by the ECM algorithm. On the group level, a one-sample *t*-test was used to assess whether the difference between the centrality maps for high and low volatility were significantly greater than zero across participants. Resulting t-values were converted to z-scores and thresholded at $p < .001$ (10 contiguous voxels).

Results

Behavioural results

fMRI session

Participants showed an overall high level of performance with a mean PR score of M_{PR} = 0.89 (*SD* = 0.06) during the fMRI session, indicating good attentiveness throughout the experiment. Out of 176 detectable sequences (not counting invalid cues), participants correctly responded to 165.73 events on average (*SD* = 12.91). Mean PR scores (Fig. 4A) did not differ significantly between experimental blocks ($F(3, 76) = 1.23$, $p = .30$). As stated above, two participants were excluded from further analyses due to their behavioural performance (standardised PR scores of z_{PR} = -1.79 and z_{PR} = -2.47, respectively).

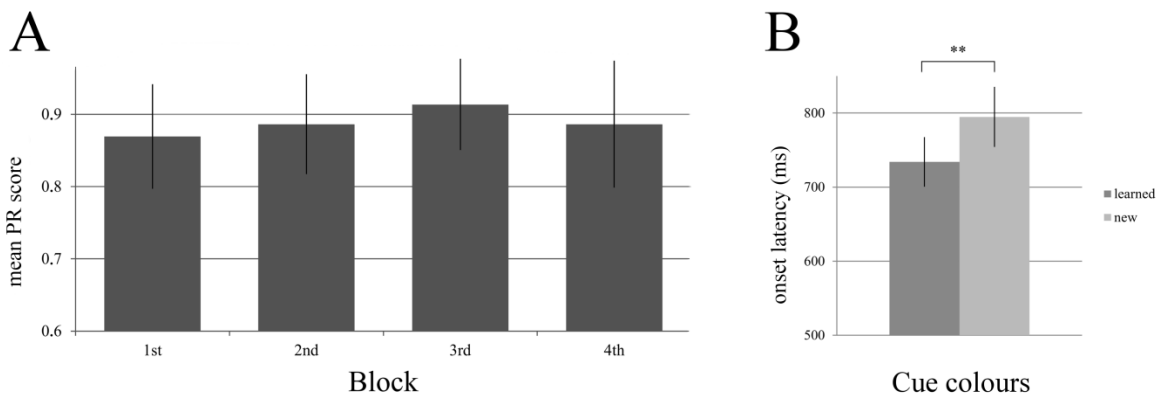

Figure 4. (A) Mean PR score for each experimental block during the fMRI session. Error bars show respective standard deviation (SD). (B) Mean onset latencies responding to learned vs new cue colours (see text) during post-measurement. Error bars show respective standard error of the mean (SEM). ** = $p < .01$

The repeated-measures ANOVA yielded a significant main effect of expectation compliance on offset latency ($F(2, 42) = 8.92$, $p = .004$, Greenhouse-Geisser-corrected). Post-hoc pairwise *t*-tests revealed participants' button releases to be significantly slower after terminated (M = 910.23 ms, SD = 365.23 ms) than after regular (M = 753.30 ms, SD = 148.87 ms, fdr-adjusted $p = .02$) as well as after extended sequences (M = 643.19 ms, SD = 231.67 ms, fdr-adjusted $p < .001$). Regular and extended sequences

did not differ significantly (fdr-adjusted p = .12). This pattern of offset latency differences appears intuitive in the sense that premature terminations unexpectedly violated the prediction of continued sequential input, thus inducing a delayed response compared to the regular condition. Critically, neither the main effect of volatility (F(1, 21) = 0.62, p = .44) nor the interaction term of *volatility X expectation compliance* (F(2, 42) = 1.87, p = .17) reached statistical significance, suggesting that participants were able to discriminate regular from manipulated sequences regardless of the respective volatility level.

Post-measurement

Participants performed equally well during the post-measurement (M_{PR} = .90, SD = 0.06) as they had during the fMRI session. Out of 40 detectable sequences (not counting invalid cues), participants correctly responded to 38.77 (SD = 2.02) sequences on average. One participant only detected 31 sequences correctly (z_{PR} = -2.54) and was excluded from further post-measurement analyses.

The post-measurement was conducted in order to assess accessibility of the signalling information provided by the cues. If participants had learned the association of cue colours and prospective ordered sequences over the course of the training and the fMRI session, they were expected to react faster to sequences beginning with established cue colours than to those starting with new colours during the post-measurement. Indeed, the corresponding t-test confirmed a significant difference between learned and new cue colours (t(20) = -3.02, p = .003, one-tailed). Participants exhibited a shorter reaction time (defined as onset latency relative to the second sequential stimulus, see above) to familiar cue colours (M = 734.07 ms, SD = 153.10) than to new cue colours just introduced during the post-measurement (M = 794.77 ms, SD = 185.94; see Fig. 4B).

fMRI results

Supporting our first hypothesis, group-level activations discernibly related to sequential terminations (*TERM > EXT*) were found in left inferior frontal gyrus (IFG) as well as in left superior frontal gyrus and the horizontal segment of the left intraparietal sulcus (hIPS, see Fig. 5A). In contrast, sequential extensions (*EXT > TERM*) were found to be distinctly reflected in activations across an extensive network comprising posterior cingulate cortex (PCC), right superior frontal sulcus (SFS), and bilateral angular gyrus (Table I).

Table I. Activation peaks, z-values, and anatomical locations for the main effect of expectation compliance *(TERM > EXT)*.

	local maxima				
	MNI				
area	x	y	z	z-value	volume (mm^3)
TERM > EXT					
left medial SFG / BA8	-6	25	44	3.88	810
left horizontal IPS	-36	-44	41	3.60	918
left IFG / BA44	-48	10	23	3.83	4023
right PCG	33	-35	74	4.07	1053
EXT > TERM					
right angular gyrus	51	-68	47	-4.34	6480
right anterior SFS	30	37	41	-3.80	2133
right STG	48	-8	-4	-4.10	2241
right BA8	39	22	50	-3.85	2241
right PCC/BA31	15	-32	41	-3.58	999
right BA40	64	-38	41	-4.17	945
left angular gyrus	-57	-65	44	-3.94	1323
right STG	48	-32	17	-3.88	1377
left STG	-51	1	-7	-4.24	2565

BA = Brodmann Area, SFG = superior frontal gyrus, IPS = inferior parietal sulcus, IFG = inferior frontal gyrus, PCG = postcentral gyrus, SFS = superior frontal sulcus, STG = superior temporal gyrus, PCC = posterior cingulate cortex.

As expected, volatility had a significant effect on checkpoints processing (CHECK HIGH > CHECK LOW). Contrary to our hypothesis, however, enhanced activation at sequential checkpoints during blocks of high volatility was not found in ACC, but in bilateral IFG and the corresponding projection area in parietal cortex, right angular gyrus / temporoparietal junction (TPJ, Fig. 5B; see Table II for coordinates).

Table II. Activation peaks, z-values, and anatomical locations for the effect of volatility on checkpoint processing (CHECK_HIGH > CHECK_LOW).

	local maxima				
	MNI				
area	x	y	z	z-value	volume (mm^3)
CHECK_HIGH > CHECK_LOW					
right TPJ / angular gyrus	36	-65	41	3.81	1296
right IFG / BA44	33	16	26	4.04	1296

TPJ = temporoparietal junction, IFG = inferior frontal gyrus, BA = Brodmann Area.

The conjunction of terminations and extensions relative to checkpoints (i.e. unexpected relative to expected events, TERM > CHECK ∩ EXT > CHECK) yielded significant activations in right SFS and bilateral inferior parietal lobe (IPL), specifically within the supramarginal gyrus (SMG, Fig. 5C; see Table III for peak coordinates). Conceptually, this joint pattern reflects the shared portion of prediction error processing (i.e. an unexpected violation of the internal model) in distinction to the qualitative differences in how the internal model is violated (i.e. having to prematurely neglect vs unexpectedly resume the sequence model, see above).

Table III. Activation peaks, z-values, and anatomical locations for the conjunction sequential terminations and extensions vs checkpoints, respectively (TERM > CHECK ∩ EXT > CHECK).

area	local maxima				
	MNI			z-value	volume (mm^3)
	x	y	z		
(TERM > CHECK) ∩ (EXT > CHECK)					
right posterior SFS / BA8	27	16	53	4.68	10071
right IPL / BA40	54	-35	50	4.19	5022
left BA10	-39	55	14	3.87	891
left IPL / BA40	-51	-35	56	4.21	1080
left BA40	-66	-32	23	4.61	5211
right BA10	30	52	20	4.24	4644
right Putamen	33	-5	2	3.71	2781

SFS = superior frontal sulcus, BA = Brodmann Area, IPL = inferior parietal lobe.

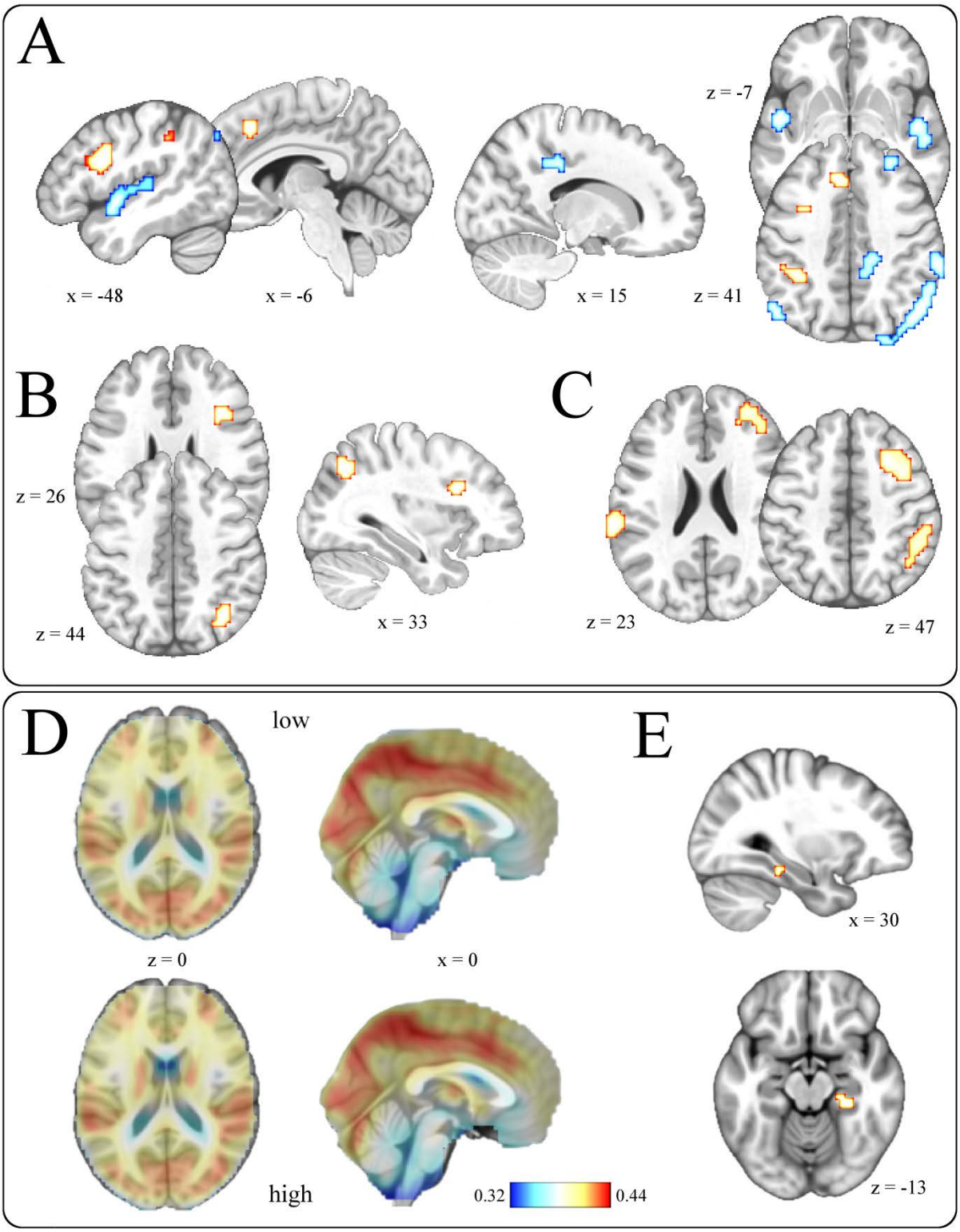

Figure 5. (A) Areas positively correlated with sequential terminations (red) and extensions (blue, contrast TERM > EXT). (B) Areas reflecting neural processing at sequential checkpoints for high (vs low) volatility (contrast CHECK_HIGH > CHECK_LOW). (C) Common activations of terminations and extensions relative to checkpoints (TERM > CHECK ∩ EXT > CHECK). (D) Group averages of eigenvector centrality for low and high volatility blocks. (E) Significantly higher centrality within the parahippocampal region for high > low volatility as revealed by a pairwise t-test.

The surprise parameter modulated neural responses in a widespread network (Table IV) including bilateral anterior-dorsal insular cortex, right anterior cingulate cortex (ACC), and right fusiform gyrus (see Supplementary Fig. 2).

Table IV. Activation peaks, z-values, and anatomical locations for the parametric effect of surprise.

	local maxima				
	MNI				
area	x	y	z	z-value	volume (mm^3)
left dorsal insula	-30	22	2	4.26	5157
right dorsal insula	30	28	2	4.48	2268
right fusiform gyrus	21	-71	-13	5.34	2079
left BA4/BA6	-45	-8	56	3.96	918
right BA40	60	-44	26	3.60	918
left SFG	-15	4	68	4.10	810
right ACC	6	25	29	3.67	1107

BA = Brodmann Area, SFG = superior frontal gyrus, ACC = anterior cingulate cortex.

Exploratory eigenvector centrality mapping

Based on the finding that volatility modulated neural processing of sequential checkpoints, we used eigenvector centrality mapping (ECM) as an exploratory tool to analyse volatility effects exceeding the reported amplitude modulations. Both high and low volatility conditions equally displayed a network of highly interconnected nodes including cingulate cortex, precuneus, basal ganglia, inferior frontal gyrus, and visual areas (Fig. 5D). Intriguingly, significantly higher eigenvector centrality was observed in the right parahippocampal region (MNI coordinates 27, -35, -13) for the high volatility condition, indicating stronger functional connections between parahippocampal areas and the other central nodes (see above) during time periods of statistical instability (Fig. 5E).

Discussion

The present fMRI study was conducted to investigate the strategic adaptation of predictive processing to different non-reward prediction error qualities and to the prediction's contextual volatility. Distinguishable activation patterns were elicited by prediction errors depending on the respective error type, lending support to a differential concept of non-reward prediction errors. In particular, we found that unexpected terminations and extensions of predicted stimulus regularities elicited increased activity in distinct brain networks. Notably, this effect was controlled for the quantitatively variable surprise level (i.e. the respective improbability) of the sampled event types. Moreover, increased activity at checkpoints for high vs low contextual volatility showed that context volatility affects predictive strategies. Thus, stable (i.e. lowly volatile) contexts allowed a full-length prediction of sequential input based on the internal model, whereas highly volatile contexts induced iterant comparisons of sensory information with the internal model. Neural processing at checkpoints was more pronounced in these unstable contexts, resulting in stepwise (rather than full model length) prediction. These results provide novel insight into adaptive prediction strategies and their respective neural underpinnings.

Qualitative differences of prediction errors

Predictions of digit sequences could be violated by termination or extension of the expected sequence length. While both types of prediction error (relative to checkpoints) commonly elicited enhanced activity in right-lateralised posterior SFS and bilateral IPL, their direct contrast yielded distinct frontoparietal activity specific to the respective prediction error type. While we tested two hypotheses for this contrast (IFG for terminated and PCC for extended sequences), we discuss further findings to suggest testable hypotheses for future studies.

The hypothesised PCC activation for extended sequences lends support to previous studies linking PCC to balancing stimulus- and memory-directed cognition (Leech et al., 2011): through high connectivity to frontoparietal circuits of cognitive control, an external focus of attention is thought to

elicit deactivation of dorsal PCC during cognitive tasks (Raichle et al., 2001; Leech et al., 2012). Here we show that an unexpected extension of sequential input, fostering the resumption of comparing incoming stimuli with the internal model, causes higher PCC activation as well. This is in contrast with terminated sequences which called for reorientation towards external stimuli and an earlier-than-expected disengagement from the internal model.

Terminated sequences correlated with neural activity within IFG (BA44, see below) whereas extensions were reflected in effects along the anterior portion of right SFS (lateral BA8/9). Evidence from the action observation literature has implicated the SFS in the processing of event boundaries (Schubotz et al., 2012), i.e., behaviourally relevant transition points in event perception. In line with the authors' interpretation of boundary-related SFS activity as a correlate of updating attention to the next stimulus, prediction error signals caused by sequential extensions presumably reflect the violation of the (expected) sequence ending: at the point of a sequential extension, participants were presented an unpredicted sequential digit when in fact expecting a random digit denoting the end of the ordered sequence (vice versa for terminated sequences). In other words, present correlates of extended sequences supposedly express a prediction error signal that ultimately results in memory-directed reorientation of attention, i.e., the resumption of the internal model.

This interpretation is substantially supported by coactivation of the angular gyrus, another component frequently associated with attentional reorientation towards salient or informative stimuli (Rushworth et al., 2001; Kincade et al., 2005; Gottlieb, 2007). The angular gyrus, specifically the dorsal portion we report for sequential extensions, has been shown to be connected to superior frontal areas via the occipitofrontal fascicle (Nelson et al., 2010, Makris et al., 2007). Functionally, one suggested role for the angular gyrus in attentional updating has been the integration of current stimuli with recent task history (Taylor et al., 2011) - a highly relevant operation for extended but not for terminated sequences. In a similar vein, O'Connor and colleagues (2010) reported expectancy violations in an attentional cueing task to be reflected in supramarginal and angular gyrus. Their

differential findings of prediction errors following old vs new items led the authors to assume that IPL lesions should affect cognitive control mechanisms especially when unexpected familiar items violate a strong expectation of novel stimuli. Our results further substantiate these suggestions, as the characteristic quality of extended sequences was precisely the observation of history-conform sequential digits when participants expected novel (i.e. random) digits.

In contrast to sequential extensions, *one specific* digit (i.e. the preceding number raised by one) was expected at the point of violation during terminated sequences. Therefore, sequential terminations can be considered violating a more specific prediction than was the case for sequential extensions. This elicited activity in a distinct frontoparietal network for terminated as compared to extended sequences, comprising left-lateralised IFG (BA44) and medial superior frontal gyrus (SFG, BA8) as well as left inferior parietal lobule (hIPS). Our finding of IFG activity increase for sequential terminations adds to consistent reports of BA44 reflecting violations of expected regularities in language syntax (Friederici & Kotz, 2003), musical structure (Maess et al., 2001), actions (Wurm & Schubotz, 2012), and abstract stimuli (Huettel et al., 2002). Contrary to an unexpected *continuation* of observed regularities (see above), these studies and our own results commonly point to a role for IFG in processing premature rule violations when regular input of certain specificity is expected.

Correspondingly, left hIPS was more strongly activated by terminated sequences, which can be explained as a prediction error signal occurring while the internal sequence model is still in progress. The horizontal segment of the IPS has consistently been reported for both numerical and non-numerical judgements of order and magnitude (Zorzi et al., 2011; Piazza et al., 2007), leading to the interpretation of hIPS as the site of the *mental number line* (Franklin & Jonides, 2008). Therefore, we consider hIPS a promising site for representing prediction errors elicited by the unexpected numeric mismatch characteristic of sequential terminations.

Predictive processing as a function of statistical context

The second main aim of the present study was to assess predictive strategies in varying statistical contexts. Processing of changes in statistical regularities per se has been demonstrated for both reward (Behrens et al., 2007) and non-reward paradigms (Tobia et al., 2012). However, it remains unclear whether or not predictions of abstract upcoming input strategically change with context (note that here, "strategically" does not imply a conscious effort). To dissociate predictions in a stable vs unstable context, the reasoning was as follows: while an implicit cue might trigger the prediction of sequential input at full length in a stable context, an unstable context might lead to a stepwise processing confirming the prediction is still valid. Recall the staircase analogy from before: in an unstable context (e.g. in dim lighting), one might be well advised to verify the initial prediction ("This flight has 13 steps") at some critical point in order not to encounter a (potentially precarious) prediction error.

Following this rationale, we investigated effects of volatility on the neural processing of possible checkpoints during prediction. Checkpoints were defined as regular events at those sequential positions where prediction errors occurred in terminated or extended sequences. Note that, by definition, prediction errors did not occur in regular sequences from which checkpoints were sampled. Right IFG showed increased BOLD activity at checkpoints within the high (vs low) volatility condition. Given the central involvement of prefrontal cortex (PFC) in flexible interactions with the environment, a process oftentimes termed *cognitive control* (Petrides, 2000; Corbetta & Shulman, 2002), enhanced prefrontal responses at *potential* violation sites might indeed be interpreted as an updating mechanism accounting for changes of statistical regularities. Previous work has shown that experimental context can be decoded from prefrontal neurons (Waskom et al., 2014), suggesting that cognitive control and decision-making benefit from representations of current context encoded in PFC. Conceivably, the use of specific vs higher-order information for context encoding in PFC depends on the respective network in which frontal sites are coactivated. Recall that a left-lateralised network comprising IFG and the numerically sensitive hIPS was found for violations of number-

specific expectations. Consolidating IFG effects for both sequential terminations and highly volatile checkpoints, the common role for prefrontal sites may be a close monitoring of structured incoming information. Depending on whether these monitoring processes lead to the detection of a specific prediction error (as in the TERM > EXT contrast) or provide vital information about the current task context (i.e. CHECK_HIGH > CHECK_LOW), respective network partners are coactivated accordingly. Support for this interpretation comes from our finding that checkpoint processing during high volatility was also found to be reflected within the right TPJ. As a direct projection site of IFG, TPJ has been established as part of a ventral network engaged in attentional control (Corbetta & Shulman, 2002; see Cabeza et al., 2008 for a review). Specifically, this network initiates a bottom-up reorientation driven by behaviourally relevant but unattended stimuli. However, an intriguing hypothesis redefining TPJ function was put forward by Geng and Vossel (2013): the authors propose contextual updating as the main role of TPJ in cognitive processing, meaning the updating of internal models of context based on new sensory information (Seghier, 2013). It is important to recall that the contrast of interest (*CHECK_HIGH > CHECK_LOW*) only contained events of regular sequences where a violation of prediction (termination or extension, respectively) was probable but did in fact not occur. Since there was no external signal initiating a change in predictive strategies, enhanced processing of checkpoints for highly volatile contexts was solely based on the internal sequence model developed through previous experience. Consequently, contextual updating as well as corresponding strategic adjustments (i.e. the use of incremental predictions in unstable environments) do not seem to require a bottom-up trigger signal but can instead be prompted by model-based expectancies alone. This suggests an extension of the understanding of TPJ functioning for paradigms where contextual updating relies on top-down generated internal models of context.

Due to the higher average surprise value for checkpoints in high vs low volatility blocks, an increase in surprise could potentially present an intuitive explanation for the reported results. Crucially, however, since the surprise parameter was modelled separately within the GLM, our findings cannot be attributed to stimulus-bound surprise but instead reflect higher-order cognitive processes

exceeding trial-by-trial variation in informational value. This is further corroborated by the fact that brain areas modulated by surprise did not overlap with the set of areas modulated by volatility at checkpoints (Fig. S2).

In sum, elevated BOLD responses within IFG and TPJ at sequential checkpoints point to an adaptive quality of abstract predictive processing that to our knowledge have not been demonstrated. Depending on the stability of statistical contexts, the predictive strategy varies with regard to how far expectations reach into the future.

Motivated by the reported BOLD amplitude effects of volatility, exploratory functional connectivity analysis (ECM) revealed eigenvector centrality of the right middle temporal gyrus (MTG) and parahippocampal region to increase during epochs of high volatility. This reflects a strengthened connectivity between the parahippocampal region and those highly interconnected frontoparietal circuits that are central for the currently employed task.

The medial temporal lobe including the hippocampal formation has been established as a crucial structure for prospective processing and pattern completion during perception (Turk-Browne et al., 2010), sequence learning (Schendan et al., 2003; Schapiro et al., 2014), and especially at points of ambiguity (Kumaran & Maguire, 2006; Ross et al., 2009; Bornstein & Daw, 2012). When multiple competing predictions with regard to the next sequential item arise under uncertainty, the MTG network is hypothesised to resolve this ambiguity, resulting in enhanced hippocampal responses (for a review, see Davachi & DuBrow, 2015). Critically, the present high volatility condition was hypothesised to intensify neural processing at ambiguous checkpoints by means of a higher proportion of sequential deviants. Therefore, the finding of strengthened functional connectivity between the parahippocampal region and central task-related structures in a highly volatile environment further corroborates the understanding of MTG as a contingency-sensitive circuitry engaged in encoding and extracting statistical information. Our results moreover suggest that this information is then employed to facilitate a context-appropriate change in predictive processing,

namely a stepwise prediction strategy for highly volatile contexts. This way, instability in the environment is supposedly compensated by more frequently comparing model-based expectations with actual sensory input. Combining the contextual updating hypothesis and MTG involvement in sequential ambiguity, enhanced overall connectivity of MTG / parahippocampus under high volatility can thus be interpreted as evaluating the validity of top-down, model-based predictions in light of incoming sensory information (Lisman, 1999; Kumaran & Maguire, 2006). Presumably, a stepwise prediction is not necessary in stable contexts, possibly due to frequent validation of the internal model (i.e. the high proportion of regular sequences) resulting in high confidence in the initial full-length prediction. As for computational efficiency and economic processing, stepwise prediction appears to be a strategic adaptation to unstable contexts in order to avoid the cost of prediction errors. One intuitive neural implementation of these stepwise predictions would be through enhanced communication between MTG and frontoparietal networks, thus enabling recourse to model information in working memory. Indeed, previous studies have demonstrated the anatomical connectivity between TPJ, associated frontal areas (IFG / lateral PFC), and MTG (Petrides & Pandya, 1999; Clower et al., 2001; Makris et al., 2005; Vincent et al., 2006). Within the scope of the contextual updating hypothesis, these connections are thought to integrate internal representations of current context information with the appropriate sensorimotor transformation necessary to respond adequately (Geng & Vossel, 2013). Strengthened MTG involvement in contexts where regular updating is beneficial suggests that the internal model is iteratively checked based on cue information retrieved from working memory.

Conclusion

Different classes of abstract prediction errors are reflected in distinct brain activation patterns, predominantly within separate frontoparietal networks. Depending on whether the respective prediction error calls for reorienting towards external stimuli or staying with the internal model,

cognitive processing is adjusted accordingly. High context volatility resulted in iterative comparisons of sensory information and the internal model instead of predicting sequences at full length. Our findings suggest that this stepwise predictive strategy is conducted through enhanced connectivity between frontoparietal circuits and the hippocampal area.

Acknowledgements

We would like to thank Christiane Ahlheim, Laura Quante, Ima Trempler, and Leon Windscheid for their valuable comments on earlier drafts of this manuscript, as well as Sarah Fromme, Irina Kaltwasser, and Monika Mertens for their help during data collection.

References

Allen TA, Salz DM, McKenzie S, Fortin NJ (2014): Nonspatial sequence coding in CA1 neurons. J Neurosci 36:1547-1563.

Bastos AM, Usrey WM, Adams RA, Mangun GR, Fries P, Friston KJ (2012): Canonical microcircuits for predictive coding. Neuron 76:695–711.

Bayer HM, Glimcher PW (2005): Midbrain Dopamine Neurons Encode a Quantitative Reward Prediction Error Signal. Neuron 47:129–141.

Behrens TEJ, Woolrich MW, Walton ME, Rushworth MFS (2007): Learning the value of information in an uncertain world. Nat Neurosci 10:1214–1221.

Benjamini Y, Hochberg Y (1995): Controlling the false discovery rate: a practical and powerful approach to multiple testing. J R Stat Soc Ser B 57:289-300.

Bonacich P (2007): Some unique properties of eigenvector centrality. Social networks 29:555-564.

Bornstein AM, Daw ND (2012): Dissociating hippocampal and striatal contributions to sequential prediction learning. Eur J Neurosci 35:1011–1023.

Cabeza R, Ciaramelli E, Olson IR, Moscovitch M (2008): The parietal cortex and episodic memory: an attentional account. Nat Rev Neurosci 9:613–625.

Clark A (2013): Whatever next? Predictive brains, situated agents, and the future of cognitive science. Behav Brain Sci 36:181–204.

Clower DM, West RA, Lynch JC, Strick PL (2001): The inferior parietal lobule is the target of output from the superior colliculus, hippocampus, and cerebellum. J Neurosci 21:6283-6291.

Corbetta M, Shulman GL (2002): Control of goal-directed and stimulus-driven attention in the brain. Nat Rev Neurosci 3:201–215.

Davachi L, DuBrow S (2015): How the hippocampus preserves order: the role of prediction and context. Trends Cogn Sci 19:92-99.

Delgado MR, Locke HM, Stenger VA, Fiez JA (2003): Dorsal striatum responses to reward and punishment: effects of valence and magnitude manipulations. Cogn Affect Behav Neurosci 3:27–38.

Den Ouden HEM, Friston KJ, Daw ND, McIntosh AR, Stephan KE (2009): A dual role for prediction error in associative learning. Cereb Cortex 19:1175–1185.

Den Ouden HEM, Daunizeau J, Roiser J, Friston KJ, Stephan KE (2010): Striatal Prediction Error Modulates Cortical Coupling. J Neurosci 30:3210–3219.

Egner T, Monti JM, Summerfield C (2010): Expectation and Surprise Determine Neural Population Responses in the Ventral Visual Stream. J Neurosci 30:16601–16608.

Fiebach CJ, Schubotz RI (2006): Dynamic anticipatory processing of hierarchical sequential events: a common role for Broca's area and ventral premotor cortex across domains? Cortex, 42:499-502.

Forman SD, Cohen JD, Fitzgerald M, Eddy WF, Mintun MA, Noll DC (1995): Improved assessment of significant activation in function magnetic resonance imaging (fMRI): Use of a cluster-size threshold. Magn Res Med 33:636-647.

Fortin, NJ, Agster KL, Eichenbaum HB (2002): Critical role of the hippocampus in memory for sequences of events. Nat Neurosci 5:458-462.

Franklin MS, Jonides J (2008): Order and Magnitude Share a Common Representation in Parietal Cortex. J Cogn Neurosci 21:2114–2120.

Friederici AD, Kotz SA (2003): The brain basis of syntactic processes: functional imaging and lesion studies. Neuroimage 20:8-17.

Friston KJ (2005): A theory of cortical responses. Philos Trans R Soc London B Biol Sci 360:815–836.

Geng JJ, Vossel S (2013): Re-evaluating the role of TPJ in attentional control: Contextual updating? Neurosci Biobehav Rev 37:2608–2620.

Gottlieb J (2007): From thought to action: the parietal cortex as a bridge between perception, action, and cognition. Neuron 53:9-16.

Harrison LM, Duggins A, Friston KJ (2006): Encoding uncertainty in the hippocampus. Neur Netw 19:535-546.

Huettel SA, Mack PB, McCarthy G (2002): Perceiving patterns in random series: dynamic processing of sequence in prefrontal cortex. Nat Neurosci 5:485–490.

Ishihara S. 1917. Test for Colour-Blindness. Tokyo: Hongo Harukicho.

Jones DS. 1979. Elementary information theory. Oxford: Oxford University Press.

Kincade JM, Abrams RA, Astafiev SV, Shulman GL, Corbetta M (2005): An event-related functional magnetic resonance imaging study of voluntary and stimulus-driven orienting of attention. J Neurosci 25:4593-4604.

Kumaran D, Maguire EA (2006): An unexpected sequence of events: mismatch detection in the human hippocampus. PLoS Biol 4:e424.

Leech R, Kamourieh S, Beckmann CF, Sharp DJ (2011): Fractionating the default mode network: distinct contributions of the ventral and dorsal posterior cingulate cortex to cognitive control. J Neurosci 31:3217–3224.

Leech R, Braga R, Sharp DJ (2012): Echoes of the Brain within the Posterior Cingulate Cortex. J Neurosci 32:215–222.

Lisman JE (1999): Relating hippocampal circuitry to function: recall of memory sequences by reciprocal dentate-CA3 interactions. Neuron 22:233–242.

Lohmann G, Müller K, Bosch V, Mentzel H, Hessler S, Chen L, Zysset S, von Cramon DY (2001): Lipsia—a new software system for the evaluation of functional magnetic resonance images of the human brain. Comput Med Imaging Graph 25:449-457.

Lohmann G, Margulies DS, Horstmann A, Pleger B, Lepsien J, Goldhahn D, Schloegl H, Stumvoll M, Villringer A, Turner R (2010): Eigenvector Centrality Mapping for Analyzing Connectivity Patterns in fMRI Data of the Human Brain. PLoS One 5:e10232.

Maess B, Koelsch S, Gunter TC, Friederici AD (2001): Musical syntax is processed in Broca's area: an MEG study. Nat Neurosci 4:540-545.

Makris N, Kennedy DN, McInerney S, Sorensen AG, Wang R, Caviness JVS, Pandya DN (2005): Segmentation of subcomponents within the superior longitudinal fascicle in humans: a quantitative, in vivo, DR-MRI study. Cereb Cortex 15:854–869.

Makris N, Papadimitriou GM, Sorg S, Kennedy DN, Caviness JVS, Pandya DN (2007): The occipitofrontal fascicle in humans: a quantitative, in vivo, DT-MRI study. Neuroimage 37:1100-1111.

Mumford D (1992): On the computational architecture of the neocortex. Biol Cybern 66:241–251.

Nelson SM, Cohen AL, Power JD, Wig GS, Miezin FM, Wheeler ME, Velanova K, Donaldson DI, Phillips JS, Schlaggar BL, Petersen SE (2010): A parcellation scheme for human left lateral parietal cortex. Neuron 67:156–170.

O'Connor AR, Han S, Dobbins IG (2010): The inferior parietal lobule and recognition memory: expectancy violation or successful retrieval? J Neurosci 30:2924–2934.

Petrides M, Pandya DN (1999): Dorsolateral prefrontal cortex: comparative cytoarchitectonic analysis in the human and the macaque brain and corticocortical connection patterns. Eur J Neurosci 11:1011-1036.

Petrides M (2000): Mapping prefrontal cortical systems for the control of cognition. In: Toga AW, Mazziotta JC, editors. Brain mapping: The systems. San Diego: Academic Press. p 159-176.

Piazza M, Pinel P, Le Bihan D, Dehaene S (2007): A magnitude code common to numerosities and number symbols in human intraparietal cortex. Neuron 53:293–305.

Raichle ME, MacLeod AM, Snyder AZ, Powers WJ, Gusnard DA, Shulman GL (2001): A default mode of brain function. Proc Natl Acad Sci USA 98:676-682.

Rao RPN, Ballard DH (1999): Predictive coding in the visual cortex: a functional interpretation of some extra-classical receptive-field effects. Nat Neurosci 2:79–87.

Rushworth MFS, Ellison A, Walsh V (2001): Complementary localization and lateralization of orienting and motor attention. Nat Neurosci 4:656-661.

Rushworth MFS, Behrens TEJ (2008): Choice, uncertainty and value in prefrontal and cingulate cortex. Nat Neurosci 11:389–397.

Rolls ET (2013): The mechanisms for pattern completion and pattern separation in the hippocampus. Front Syst Neurosci 7:74.

Ross RS, Brown TI, Stern CE (2009): The retrieval of learned sequences engages the hippocampus: Evidence from fMRI. Hippocampus 19:790-799.

Schapiro AC, Gregory E, Landau B, McCloskey M, Turk-Browne NB (2014): The Necessity of the Medial Temporal Lobe for Statistical Learning. J Cogn Neurosci 26:1736–1747.

Schendan HE, Searl MM, Melrose RJ, Stern CE (2003): An fMRI Study of the Role of the Medial Temporal Lobe in Implicit and Explicit Sequence Learning. Neuron 37:1013–1025.

Schiffer AM, Ahlheim C, Wurm MF, Schubotz RI (2012): Surprised at all the entropy: hippocampal, caudate and midbrain contributions to learning from prediction errors. PloS One 7:e36445.

Schubotz RI, Korb FM, Schiffer AM, Stadler W, von Cramon DY (2012): The fraction of an action is more than a movement: Neural signatures of event segmentation in fMRI. Neuroimage 61:1195–1205.

Schultz W (1998): Predictive reward signal of dopamine neurons. J Neurophysiol 80:1–27.

Seghier M (2013): The Angular Gyrus: Multiple Functions and Multiple Subdivisions. Neuroscientist 19:43–61.

Silvetti M, Seurinck R, Verguts T (2013): Value and prediction error estimation account for volatility effects in ACC: a model-based fMRI study. Cortex 49:1627–1635.

Snodgrass JG, Corwin J (1988): Pragmatics of measuring recognition memory: applications to dementia and amnesia. J Exp Psychol 117:34.

Strange BA, Duggins A, Penny W, Dolan RJ, Friston KJ (2005): Information theory, novelty and hippocampal responses: unpredicted or unpredictable? Neural Netw 18:225–230.

Taylor PCJ, Muggleton NG, Kalla R, Walsh V, Eimer M (2011): TMS of the right angular gyrus modulates priming of pop-out in visual search: combined TMS-ERP evidence. J Neurophysiol 106:3001–3009.

Tobia MJ, Iacovella V, Davis B, Hasson U (2012): Neural systems mediating recognition of changes in statistical regularities. Neuroimage 63:1730–1742.

Turk-Browne NB, Scholl BJ, Johnson MK, Chun MM (2010): Implicit perceptual anticipation triggered by statistical learning. J Neurosci 30:11177–11187.

Ullsperger M, Harsay HA, Wessel JR, Ridderinkhof KR (2010): Conscious perception of errors and its relation to the anterior insula. Brain Struct Funct 214:629-643.

Vincent JL, Snyder AZ, Fox MD, Shannon BJ, Andrews JR, Raichle ME, Buckner RL (2006): Coherent spontaneous activity identifies a hippocampal-parietal memory network. J Neurophysiol 96:3517–3531.

Waskom ML, Kumaran D, Gordon AM, Rissman J, Wagner AD (2014): Frontoparietal Representations of Task Context Support the Flexible Control of Goal-Directed Cognition. J Neurosci 34:10743–10755.

Wurm MF, Schubotz RI (2012): Squeezing lemons in the bathroom: Contextual information modulates action recognition. Neuroimage 59:1551-1559.

Zorzi M, Di Bono MG, Fias W (2011): Distinct representations of numerical and non-numerical order in the human intraparietal sulcus revealed by multivariate pattern recognition. Neuroimage 56:674–680.

OnlineSuppl_Text

Click here to download Suppl. material for online publication only: Cortex_Supplement_Kluger_Schubotz_170215.pdf

OnlineSuppl_Fig_S1

Click here to download Suppl. material for online publication only: Rev_FigS1_Kluger_Schubotz_170215.tif

OnlineSuppl_Fig_S2

Click here to download Suppl. material for online publication only: Rev_FigS2_Kluger_Schubotz_170215.tif